

Characterizing and Mapping Mangrove Species Using Spectral Signatures in the Red Sea, Egypt

Asmaa H. Mohammed¹, Eslam Farg², Mahmoud H. Hanafy³, Sayed A. Mohamed^{4*}

¹Marine Sciences Department, National Authority for Remote Sensing and Space Sciences, (NARSS), Cairo 11769, Egypt

²Agriculture applications Department, National Authority for Remote Sensing and Space Sciences, (NARSS), Cairo 11769, Egypt

³Marine Sciences Department, Science college, Suez Canal University, Egypt

⁴Data Reception, Analysis, and Receiving Station Affairs Division, National Authority for Remote Sensing and Space Sciences (NARSS), Cairo 11769, Egypt

*Corresponding author: asmahassan@narss.sci.eg

ARTICLE INFO

Article History:

Received: Nov. 2, 2024

Accepted: Nov. 17, 2024

Online: Nov. 18, 2024

Keywords:

Mangroves,
Halophytes,
Spectral signatures,
Unmixing classification,
Egyptian Red Sea

ABSTRACT

Mangrove environments have garnered attention in recent years as a result of their substantial contribution to the earth's dynamic. Its function in carbon sequestration within coastal sediments helps alleviate climate change. Mangrove ecosystems, characterized by various tree species, face numerous threats and require continuous monitoring for conservation efforts, which can be facilitated by remote sensing. Biodiversity monitoring and the detection of different species demand highly specific techniques. This study introduces a comprehensive analysis of *in situ* spectral signatures for two mangrove species found in Egypt. We assessed these spectral signatures and organized them into a spectral library to classify high-resolution Pleiades Neo satellite images using linear unmixing techniques to differentiate the mangrove species. The results were significant, allowing us to distinguish five halophyte coastal species and accurately identify the two mangrove species, *Avicennia marina* and *Rhizophora mucronata*, with an accuracy assessment of 89.83%.

INTRODUCTION

Mangroves are the primary type of coastal vegetation distributed along the eastern and western shores of the Red Sea, found at tropical and subtropical latitudes, reaching the Nabq area in Egypt, which represents the northernmost extent of mangroves worldwide (Shaltout *et al.*, 2005). Mangroves are type of halophytes plants that survive in the harsh environmental conditions of semi-arid areas and form aggregations to forests along coastal. According to tidal range, they are situated from narrow to wide belt in the Red Sea (Hickey *et al.*, 2017).

Mangroves play a vital ecological role as one of the most productive marine habitats. The mangroves trees are important shelters and feeding nursery for both land and marine dwellers. The stands of mangroves protect the coastal from erosion and storms (Afefe *et al.*, 2019). Globally, mangrove forests play a crucial role in the carbon cycle, being one of the most carbon-rich ecosystems. Their average total carbon storage per unit area is five times greater than that of other forest types. There are approximately 56 mangrove species worldwide (Spalding, 2010). In the Red Sea, about 4 species can be found (Kassas & Zahran, 1967; PERSGA, 2004). In addition, *Avicennia marina* is the most abundant mangrove species, followed by small areas of well-grown *Rhizophora mucronata*, which have been recorded in several Red Sea countries: Egypt (Kassas & Zahran, 1967; Galal, 2003), Djibouti (Kassas & Zahran, 1967; Witsen, 2012), Yemen (PERSGA, 2004), Eritrea (Hailemichael, 2015), and Saudi Arabia (Almahasheer *et al.*, 2016). Except in Sudan, where *Avicennia marina* is the only mangrove species present (Sabeel, 2015), the two species, *Rhizophora mucronata* and *Bruguiera gymnorrhiza*, are considered extinct (Sabeel, 2015). Additionally, two other species, *Ceriops tagal* and *Bruguiera gymnorrhiza*, have been recorded but are very limited in the southern Red Sea, specifically in Djibouti (Kassas & Zahran, 1967; Galal, 2003; PERSGA, 2004; FAO, 2007) and Eritrea (Hailemichael, 2015).

According to the NARSS project (Mohammed, 2023), which mapped the current mangrove areas along the Egyptian Red Sea shores, 35 locations of mangrove trees cover about 600 hectares. The coverage ranges from small, scattered trees to large stands with complete ecosystems. *Avicennia marina* is common at all sites, while *Rhizophora mucronata* coexists with *Avicennia* spp. in the southern sector of Halayeb and Shalateen (Galal, 2003; Mohammed, 2023). Additionally, terrestrial halophyte plants grow adjacent to the mangroves.

Remote sensing technology has been employed to identify and map mangrove forest distribution. Due to the nature of mangrove mud sedimentation, remote sensing is more effective for observing and monitoring these areas than traditional fieldwork (Green *et al.*, 1998; Fouda, 2009). One technique involves establishing a spectral library for coastal vegetation, which aids in discriminating between different mangrove species (Kamaruzaman & Kasawani, 2007; Ajithkumar *et al.*, 2008; Xu *et al.*, 2019). The reflectance of vegetation depends on the reflectance and transmittance of leaves, which are responsible for the main spectral signatures. Healthy leaves have different reflectance properties, especially in the visible and near-infrared regions, compared to unhealthy ones. These differences are crucial for distinguishing between species using the spectral library (Kamaruzaman & Kasawani, 2007; Wang & Sousa, 2009).

Classifying remotely sensed data into thematic maps remains a challenge due to various factors, such as landscape complexity, selected remote sensing data, and the

algorithms used for image processing and classification. One advanced classification method is linear spectral unmixing, which assumes that the reflectance of a pixel is the sum of the end-member spectra, scaled in proportion to the coverage of each end-member within the pixel, based on spectral derivatives and hyperspectral data (Kutser *et al.*, 2005; Wang *et al.*, 2017; Taureau *et al.*, 2019).

This study aimed to determine the spectral properties of two mangrove species and alternative vegetation to identify significant wavelengths for distinguishing between the mangrove species along the Egyptian coast. Additionally, it employed linear unmixing classification techniques (sub-pixel) for further mapping of mangroves using high-resolution Pleiades Neo satellite images and an *in-situ* spectral library, representing a novel approach for mapping mangroves in Egypt.

MATERIALS AND METHODS

1. Study area

The study location was chosen in Shalateen Province due to the presence of both mangrove species, *Avicennia marina* and *Rhizophora mucronata*. The area is located between 22° 58' and 22° 53' North and between 35° 40' and 35° 44' East of Shalateen City (Fig. 1). This remote region is inhabited by the local Ababda community, who utilize it for grazing purposes.

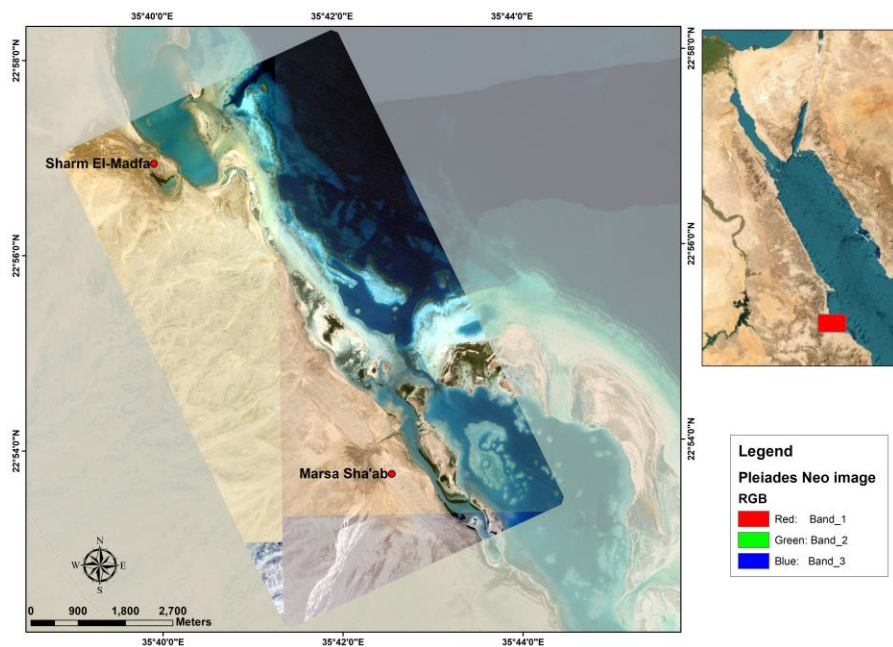


Fig. 1. Location of the study area

2. Collecting *in-situ* spectral measurement for mangrove species

The spectral signatures for five different halophyte vegetation species including two different mangrove species were measured as reflectance. The measurements were obtained by using a portable “ASD Field Spec_4 instrument” (Fig. 2). The portable Spectro-radiometer is capable to record spectral range of 350–2500nm by a rapid data collection time of 0.2 second per spectrum. It has spectral resolution of three nm in visible wavelength range (350-700nm) and NIR and SWIR from 750 to 2500nm. In addition, leaf pigments were measured using an *in situ* chlorophyll meter (SPAD).



Fig. 2. Measurement on field with different instruments; **a**, Spectroradiometer, **b**, Chlorophyll meter

2.1. Analysis for filed measurements

First, the spectral signatures of different species were organized and aligned with the corresponding wavelength ranges. In this study, the following scale ranges were used: coastal range (350–450nm), blue (451–510nm), green (511–580nm), yellow (581–630nm), red (631–690nm), red-edge (691–750nm), NIR (751–1040nm), and SWIR1 and SWIR2 (1040–2500nm). These end-member wavelengths were arranged according to their respective color ranges.

2.2. Statistics analysis

The spectral variability of two mangrove species and three other vegetation species was analyzed using ANOVA to identify regions of the electromagnetic spectrum where the colors differ significantly. The one-way analysis of variance (ANOVA) was conducted, followed by Tukey's post hoc test across each band to verify differences among species means (Tukey, 1977; Mason *et al.*, 2003).

3. Satellite imagery

The Pleiades Neo image was acquired on January 20, 2024 (Fig. 2). The dataset has a spatial resolution of 50cm for panchromatic images and approximately 1.8 meters for multispectral images. The spectral bands range from Deep Blue (400–450nm), Blue (450–520nm), Green (530–590nm), Red (620–690nm), Red Edge (700–750nm), to Near-Infrared (770–880nm), with a panchromatic range of 450–800nm.

3.1. Preprocessing analysis

The pre-processing steps included: A) re-projection of the imagery product to rectify the coordinates to WGS84, zone 37; B) layer stacking to fuse the panchromatic image with the six multispectral bands, resulting in a pixel spatial resolution of 0.50m. Finally, the image was subset using ENVI software version 5.3.

3.2. Linear spectral unmixing classification

The linear spectral unmixing technique, has been applied on calibrated Pleiades image of Shalateen area by using the linear spectral unmixing model of ENVI 5.3. The classification was based on the *in-situ* spectral library of coastal mangrove vegetation. Spectral unmixing is the process of decomposing the measured spectrum of a mixed pixel into a set of distinct endmember spectra and their corresponding fractions (abundances), which represent the proportion of each endmember in the pixel (**Horwitz, 1971**).

3.3. Accuracy assessment

The final thematic results were assessed using a confusion matrix comparing the observed data from the field with the classified map classes. The agreement between the map and the ground truth is represented by the diagonals of the matrix, indicating commission and omission errors (**Tharwat, 2018**). Additionally, the error matrix can be used to compute statistical measures such as the Kappa standard deviation, Kappa variance, and Kappa coefficient of agreement, defined by the formula:

$$K = (\text{observed accuracy} - \text{chance agreement}) / (1 - \text{chance agreement})$$

RESULTS

The spectral properties of two existing mangrove species, *Avicennia marina* and *Rhizophora mucronata*, were studied using a spectroradiometer (ASD). The chlorophyll concentration in the leaves of different mangrove species varied between 0.41 and 0.67mg g⁻¹, with the minimum found in *Avicennia marina* and the maximum in *Rhizophora mucronata*. *Rhizophora mucronata* exhibited high reflectance in the visible range, which then decreased in the SWIR range. In contrast, *Avicennia* sp. showed higher reflectance in the SWIR bands (Fig. 3).

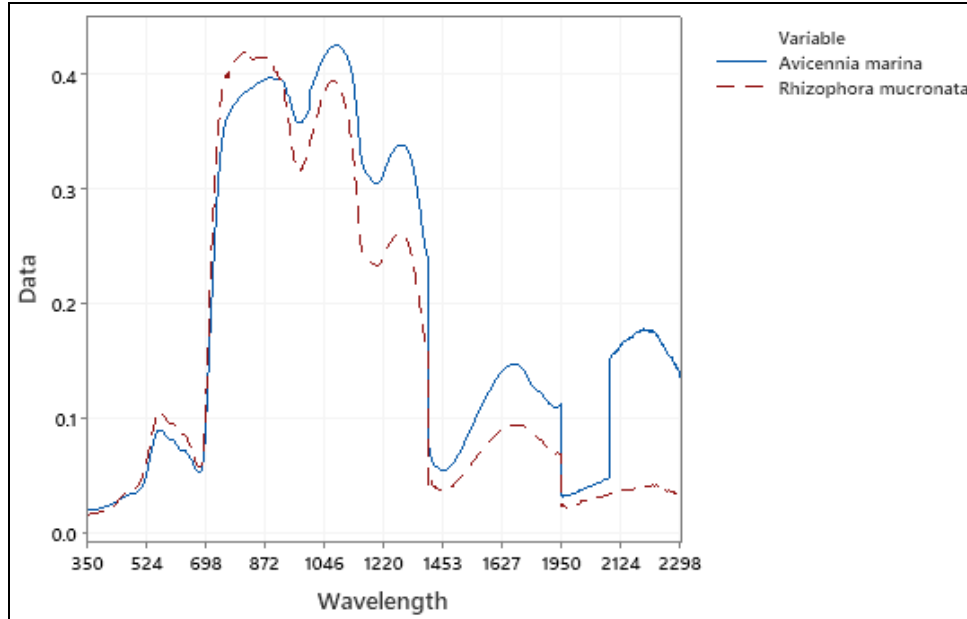


Fig. 3. The spectral signature of two mangrove species

The mangrove trees in many areas are surrounded by other vegetation and shrubs, which were also measured to distinguish the different spectral signatures of all elements in the area, including mangrove trees, natural vegetation, and the background of water and sand. Fig. (4) shows the spectral signatures of different end members of coastal halophytes, highlighting the two mangrove species, which exhibit different reflectance compared to other vegetation. Specifically, *Atriplex* sp. and *Limonium* sp. reflect lower values than the mangroves, while *Zygophyllum* sp. also shows low reflectance.

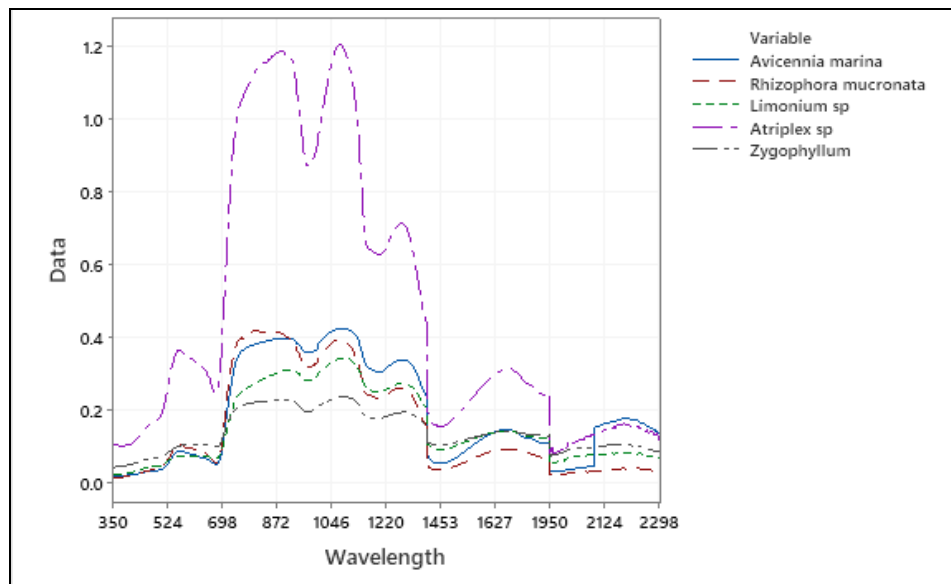


Fig. 4. The spectral signature of coastal halophytes with mangrove species

Characterizing and Mapping Mangrove Species Using Spectral Signatures in the Red Sea, Egypt

The spectral signatures of the two mangrove species were analyzed using a one-way ANOVA to calculate the significant differences between them according to wavelength ranges. Fig. (5) shows the significant differences between the two mangrove species across various spectral bands, from visible light to the shortwave infrared (SWIR1 and SWIR2). Notably, *Rhizophora* sp. exhibited high significance in the Red Edge and SWIR1 bands.

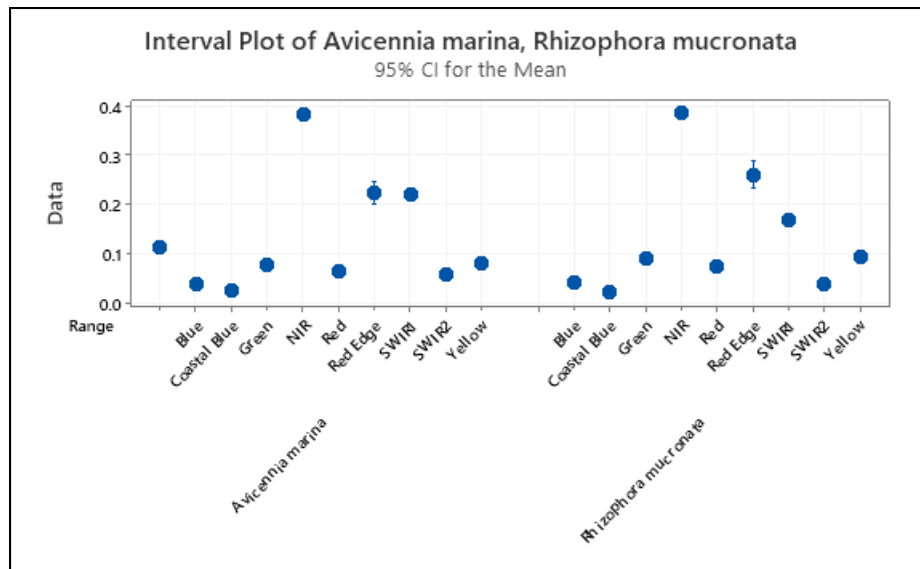


Fig. 5. The interval plot of two mangrove species

According to Tukey's ANOVA analysis, the mean reflectance values between the mangrove species were significantly different across several bands, including green, yellow, red, red edge, NIR, SWIR1, and SWIR2. The mean values were 0.170 for *Avicennia* and 0.157 for *Rhizophora*, respectively, with a standard deviation of 0.14, as shown in Table (1). The T-value and simultaneous tests, represented in Fig. (6), indicate the significance between the two mangrove species. Additionally, Fig. (7) confirms the differences between the two mangrove species based on the pooled standard deviation interval.

Table 1. Tukey pairwise comparisons, one-way ANOVA

Factor	N	Mean	Grouping	
<i>Avicennia marina</i>	1951	0.17027	A	
<i>Rhizophora mucronate</i>	1743	0.15714		B

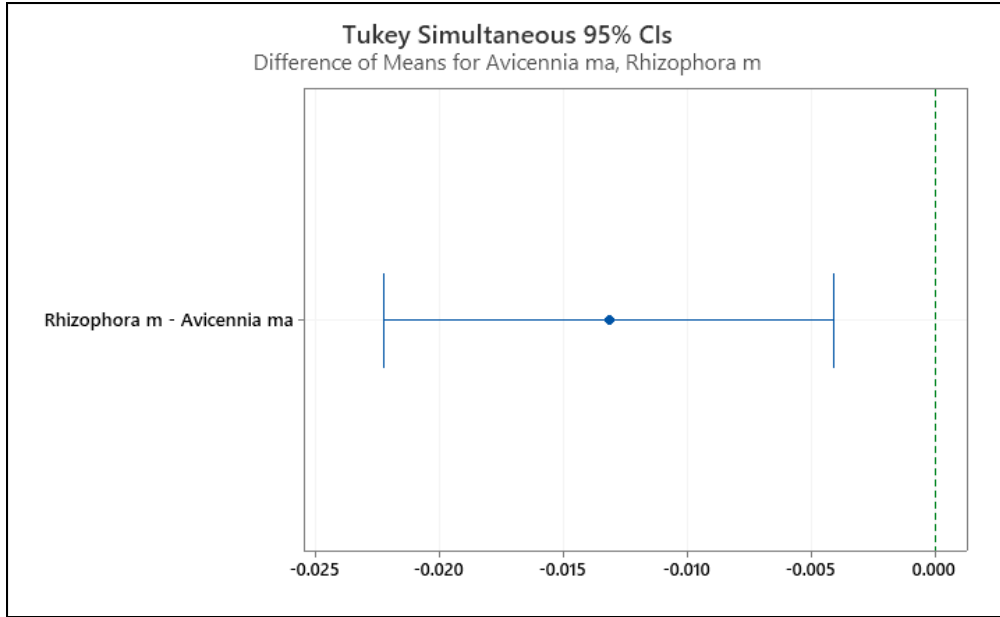


Fig. 6. Tukey simultaneous tests for differences of means of two mangrove species

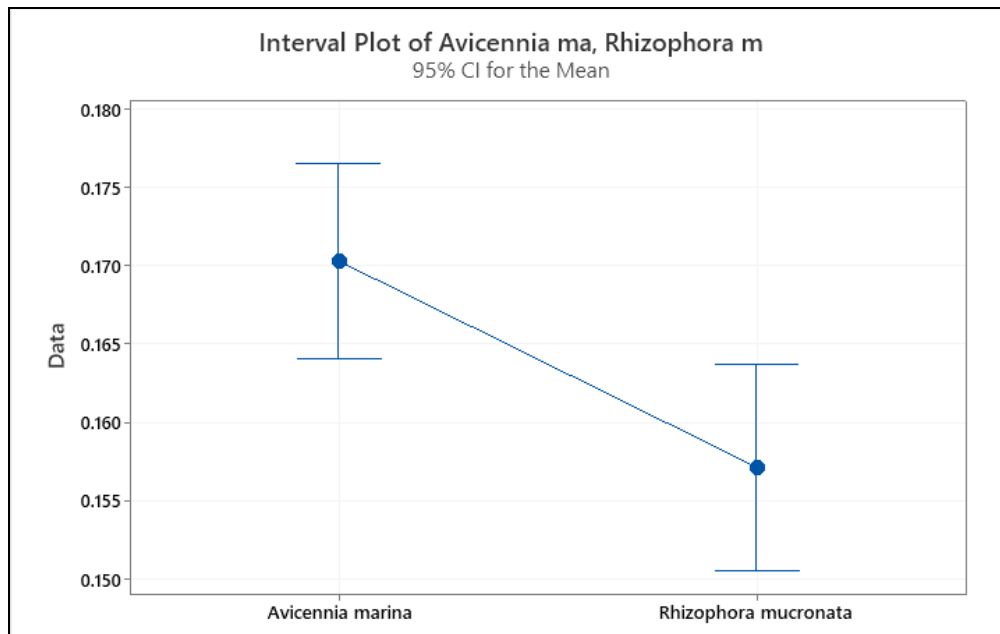


Fig. 7. The pooled standard deviation interval of two different mangrove species

The results of classified high resolution satellite image

Based on the linear spectral unmixing of the classified image of the study area, which contains the two mangrove species, results are plotted in Fig. (8). The discrimination of different mangrove species is enhanced by linear spectral unmixing, utilizing *in situ* endmember spectral signatures. Fig. (9) illustrates the stand of *Avicennia*

Characterizing and Mapping Mangrove Species Using Spectral Signatures in the Red Sea, Egypt

sp., showcasing various growth forms of trees. The classification tool differentiates larger trees from smaller ones and assesses the density of stands, ranging from high to low density of scattered trees. Furthermore, Fig. (10) demonstrates the capability of high-resolution satellite imagery to analyze mangrove density and species differentiation. The lower figure shows that both mangrove species are separated by different values, alongside other halophyte shrubs.

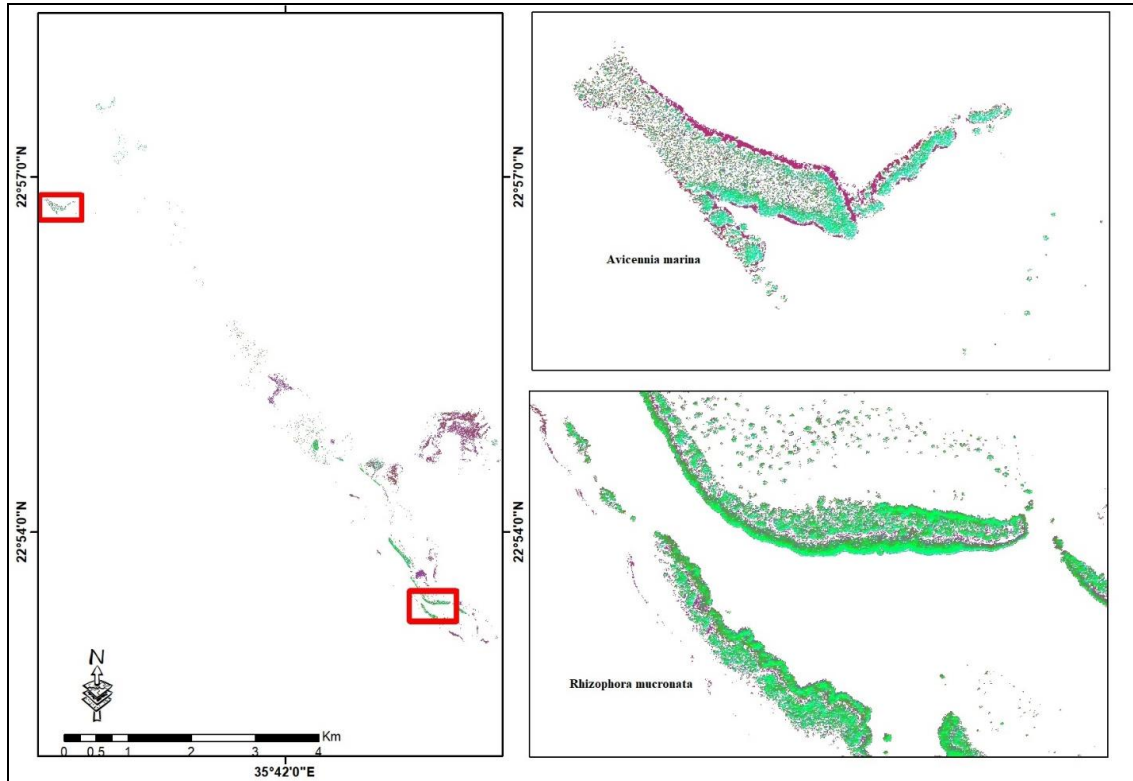


Fig. 8. Mangroves mapped from Pleiades Neo image using unmixing classification technique

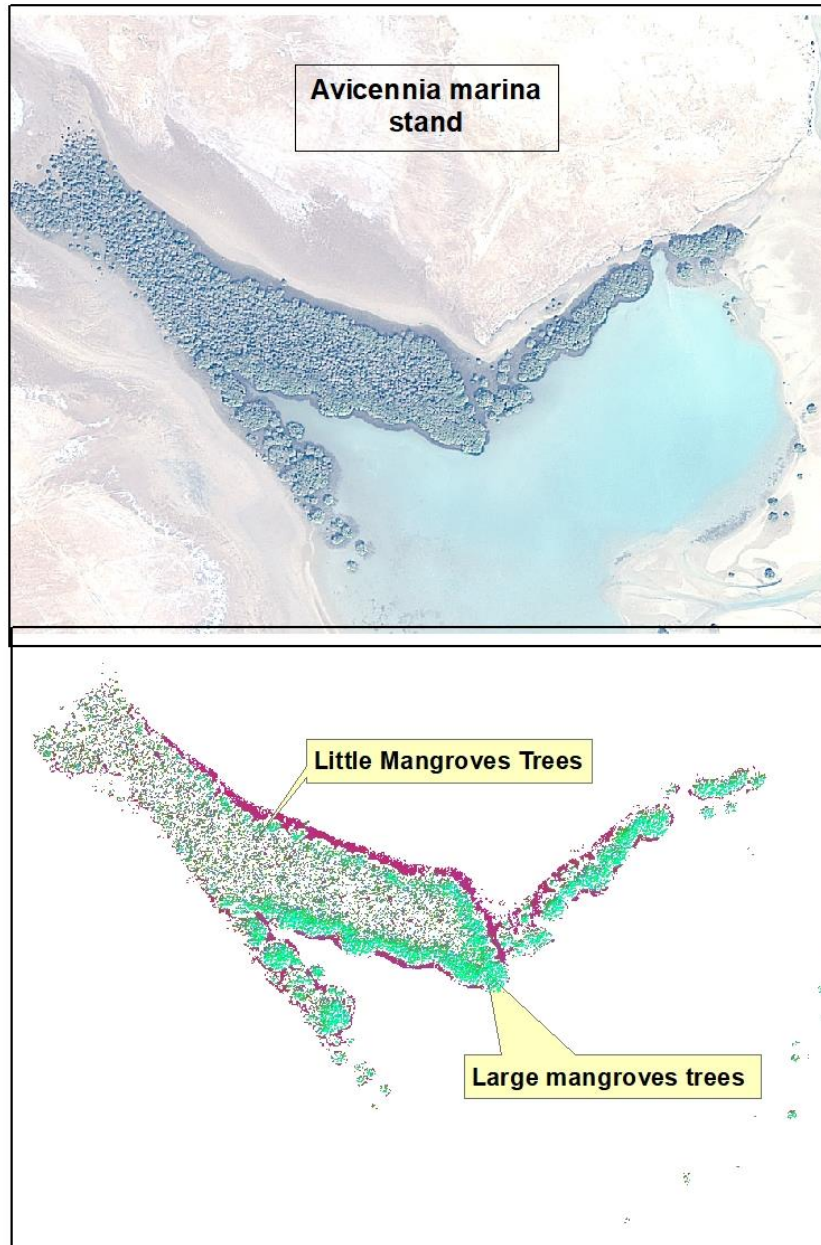


Fig. 9. *Avicennia* sp. mangroves as shown in the Pleiades Neo image at the top, with the lower portion depicting the same area mapped using unmixed classification

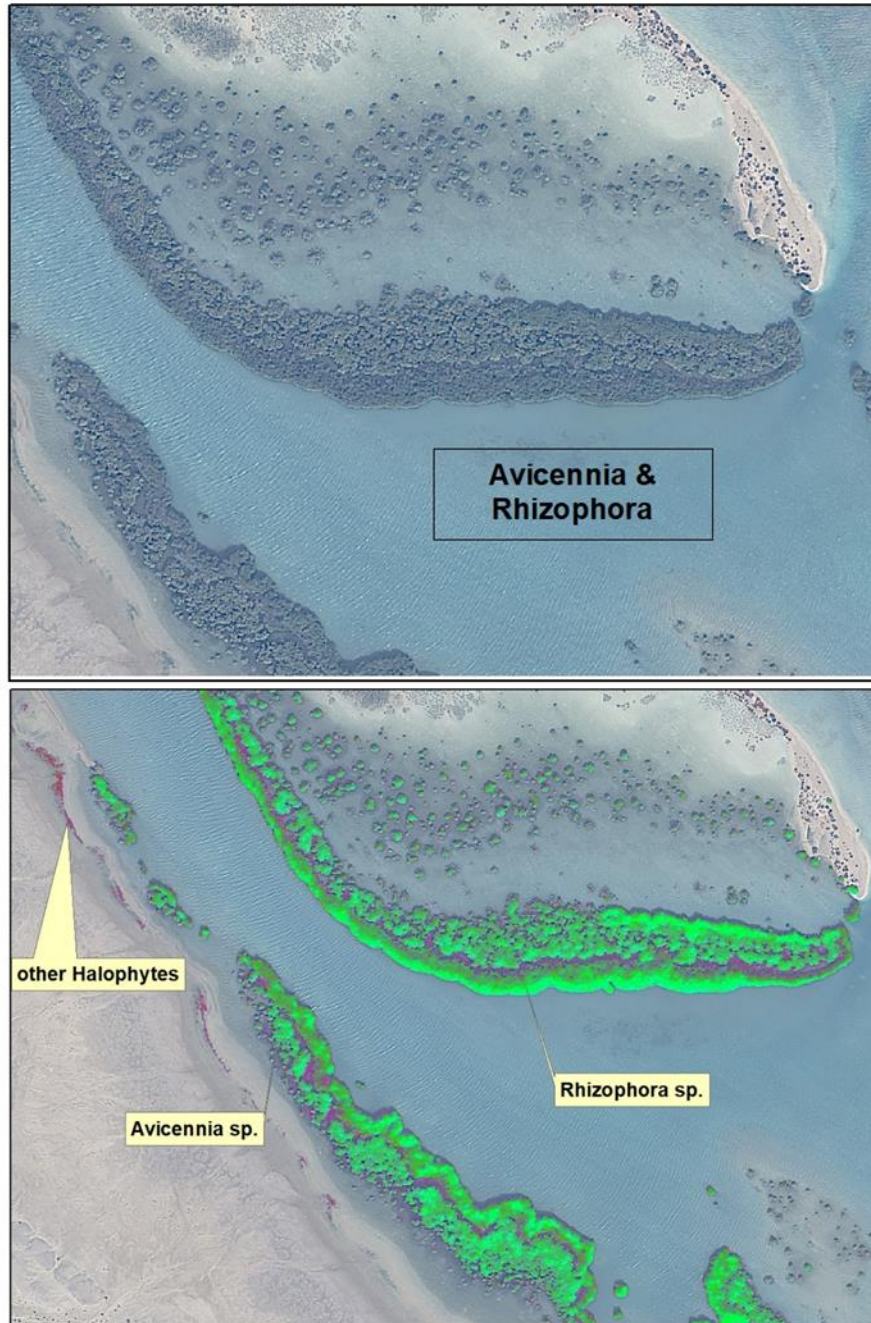


Fig. 10. Two mangroves' species interpreted from Pleiades Neo image at top, and lower mapped by using unmixing classification technique

Accuracy assessment

The overall accuracy of the classification results is 89.83%, with *Avicennia* sp. achieving a higher detection accuracy of 89.9% compared to *Rhizophora* sp., which has an accuracy of 88.8% (Table 2). Additionally, the Kappa coefficient is 0.847, indicating a reasonable level of agreement for the output classes.

Table 2. The accuracy assessment table (confusion matrix)

Classes	<i>Avicennia</i> sp	<i>Rhizophora</i> sp	Other halophytes	Classification overall	Producer accuracy
<i>Avicennia</i> sp	107	5	7	119	89.9%
<i>Rhizophora</i> sp	5	104	8	117	88.8%
Other halophytes	7	3	98	108	90.7%
Truth overall	119	112	113	344	
User accuracy	89.9%	92.8%	86.7%	89.83%	

DISCUSSION

Given that the chlorophyll pigmentation concentrations were high on *Rhizophora* sp. than *Avicennia* sp., resulting from the absorption of more amount of sunlight for photosynthetic processes, the species with high pigmentation absorb more light and reflect less. The studies by **Kamaruzaman and Kasawani (2007)**, **Ajithkumar *et al.* (2008)** and **Xu *et al.* (2019)** measured spectral reflectance for different mangrove species and indicated that chlorophyll concentration is one of the major factors responsible for determining the reflectance pattern of the plant communities. In addition, *Rhizophora* sp. has larger leaves compared to *Avicennia* sp., which indicates a distribution of different pigments, including chlorophyll, within the main wavelength ranges from 525 to 750nm, reflecting the physical activities of the leaves (**Gitelson *et al.*, 2003**; **Zhu *et al.*, 2020**; **Rahmandhana *et al.*, 2022**). The effect of salinity on *Avicennia* sp. leaves increases their thickness, which in turn affects the spectral signatures in the red and NIR ranges, resulting in decreased reflectance (**Al-Jubouri & Wheib, 2020**).

Other halophytes, such as *Atriplex* sp., exhibit higher reflectance than mangroves, which is related to lower chlorophyll content in their leaves due to salinity (**Grašič *et al.*, 2017**; **Al-Jubouri & Wheib, 2020**). The spectral signatures of mangrove trees show different reflectance compared to the background water, related to the pigment bio-content in the trees (**Wang & Sousa, 2009**; **Lee *et al.*, 2019**).

The spectral unmixing technique provides fractional images of the two mangrove species (endmembers), offering specific details about image composition because the analysis operates at a sub-pixel level. This approach is helpful for distinguishing different species and their various growth forms. The classification results specify distinct spectral signatures for different mangrove species, enabling accurate mapping based on their spectral properties (**Thayn, 2020**; **Devy *et al.*, 2022**). Spectral unmixing offers numerous

benefits for the assessment, monitoring, and management of coastal ecosystems (**Kamal & Phinn, 2011; Taureau et al., 2019**) because fractional endmember images provide more detailed information about stand composition than traditional interpretations or pixel-scale classifications.

Different mangrove species have unique reflectance characteristics (**Arfan et al., 2015; Tran et al., 2022**), particularly in the visible and SWIR ranges. Various indices are employed to extract vegetation in general and mangroves specifically, which are effective for mapping but do not differentiate between species. Furthermore, linear unmixing confirms high accuracy in discriminating the two mangrove species within the same area. A variety of classification methods have been used for mangroves (**Sanjot et al., 2022; Armanda et al., 2024; Felegari et al., 2024**), ranging from pixel-based classification to spectral angle mapper algorithms and artificial intelligence tools. The linear unmixing classification method is considered highly precise for mapping mangroves (**Kanniah et al., 2007; Ghosh & Chakravorty, 2020; Thayn, 2020; Lombard & Andrieu, 2021**).

CONCLUSION

This study identified five species of halophytes based on their spectral signatures along the Red Sea coastline. Field measurements of spectral signatures enabled linear unmixing classification to distinguish between the two types of mangroves present on the southern Egyptian Red Sea coast. The spectral signatures of the two mangrove species, *Avicennia* sp. and *Rhizophora* sp., exhibited significant differences, particularly in the red, NIR, and SWIR ranges. The high-resolution satellite imagery from Pleiades Neo demonstrated the capability for mapping and species-specific mangrove discrimination with an accuracy of about 90%. Future research should focus on evaluating the impact of salinity accumulation on the leaves of mangrove species and its effects on mapping results.

REFERENCES

- Afele, A.; S Abbas, M.; A Khedr, A.-H. and E Hatab, E.-B.,** (2019). Physical and chemical characteristics of mangrove soil under marine influence. A case study on the Mangrove Forests at Egyptian-African Red Sea Coast. *Egypt. J. Aquat. Biol. Fish.* 23, 385–399.
- Andrews, F.W.** (1950). The flowering plants of Anglo-Egyptian Sudan. Sudan Government.
- AL-Jubouri A.K.S., and Wheib K.A.,** (2020). Effect of soil salinity on spectral reflectance of Red and Nir wavelengths in Al-Salamiyat project. *Plant Archives* Volume 20 No. 1, 2020 pp. 1359-1365.

- Almahasheer, H.; Aljowair, A.; Duarte, C. M. and Irigoien, X.** (2016). Decadal stability of Red Sea mangroves. *Estuar. Coast. Shelf Sci.* 169, 164–172. doi: 10.1016/j.ecss.2015.11.027
- Ajithkumar, T. T.; Thangaradjou, T. and Kannan, L.** (2008). Spectral reflectance properties of mangrove species of the Muthupettai mangrove environment, Tamil Nadu. *Journal of Environmental Biology*, 29(5), 785-788.
- Arfan, A.; Toriman, M.E.; Maru, R.; Nyompa, S.; and Uca** (2015). Reflectance Characteristic of Mangrove Species using Spectroradiometer HR-1024 in Suppa Coast, Pinrang, South Sulawesi, Indonesia. *Asian Journal of Applied Sciences*, Volume 03 – Issue 05.
- Armanda; Agus, S. B. and Gaol, J. L.,** (2024). Classification and Distribution of Mangrove Genus Using Multispectral Unmanned Aerial Vehicle (UAV) In the Waters of Lancang Island, Kepulauan Seribu, Indonesia. *JGEET Vol 9 No 2*.
- Devy, M.; Sanjaya, H.; Irawan, L.; Astina., I.; Sadmono, H. and Andayani, A.,** (2022). Large-Extent Mangrove Species Mapping Using Landsat 9 OLI-2: A Subpixel Analysis. 130-136. doi: 10.1109/AGERS56232.2022.10093313
- FAO (Food and Agriculture Organization of the United Nations)** (2007). *The World's Mangroves 1980-2005. FAO Forestry Paper 153*.
- Felegari, S.; Moravej, K.; Sharifi, A. and Dansh-Yazdi, M.,** (2024). Utilizing Multimodal Satellite Imagery for Enhanced Mangrove Species Classification by using Label Distribution Learning.
- Fouda, M. M.** (2009). "Fourth National Report Egypt for CBD. NCS."
- Galal, N.S.** (2003). Status of Mangroves in the Arab Republic of Egypt (Draft Report). PERSGA, Jeddah.
- Gitelson, A.; Gritz, Y. and Merzlyak, M.,** (2003). Relationships between leaf chlorophyll content and spectral reflectance and algorithms for non-destructive chlorophyll assessment in higher plant leaves. *Journal of Plant Physiology*. Volume 160, Issue 3, Pages 271-282. ISSN 0176-1617, <https://doi.org/10.1078/0176-1617-00887>.
- Ghosh, D., and Chakravorty, S.** (2020). Change detection of tropical mangrove ecosystem with subpixel classification of time series hyperspectral imagery. *Artificial intelligence techniques for satellite image analysis*, 189-211.
- Grašič, M.; Budak, V.; Klančnik, K.; et al.,** (2017). Optical properties of halophyte leaves are affected by the presence of salt on the leaf surface. *Biologia* **72**, 1131–1139. <https://doi.org/10.1515/biolog-2017-0125>
- Green, E. P.; Clark, C. D.; Mumby, P. J.; Edwards, A. J. and Ellis, A. A.,** (1998). Remote sensing techniques for mangrove mapping. *International Journal of Remote Sensing*, 19(5), 935-956.
- Hailemichael, M.,** (2015). Mangrove forest extent and status along the Eritrean Red Sea coast. MSc. Dep. of Bio., Uni. Bergen. 80pp

- Hickey, S. M.; Phinn, S. R.; Callow, N. J.; Van Niel, K. P.; Hansen, J. E. and Duarte, C. M.** (2017). Is climate change shifting the poleward limit of mangroves? *Estua. Coasts* 40, 1215–1226. doi: 10.1007/s12237-017-0211-8
- Horwitz, H.M.; Nalepka, R.F.; Hyde, P.D.; and Morgenstern, J.P.** (1971). Estimating the proportions of objects within a single resolution element of a multispectral scanner. The 7th International Symposium on Remote Sensing of Environment, Ann Arbor, Michigan, pp. 1307-1320.
- Kanniah, K. D.; Wai, N. S.; Shin, A. and Rasib, A. W.** (2007). Per-pixel and sub-pixel classifications of high-resolution satellite data for mangrove species mapping. *Appl. GIS*, 3(8), 1-22.
- Kamal M, and Phinn S.** (2011). Hyperspectral Data for Mangrove Species Mapping: A Comparison of Pixel-Based and Object-Based Approach. *Remote Sensing*. 3(10):2222-2242. <https://doi.org/10.3390/rs3102222>
- Kassas, M. and Zahran, M.A.** (1967). On the ecology of the Red Sea salt marshes, Egypt. *Ecological Monographs* 37(4): 297-315.
- Kamaruzaman, J. and I. Kasawani,** (2007). Imaging spectrometry on mangrove species identification and mapping in Malaysia. *WSEAS Trans. Biol. Biomed.*, 4: 118-126.
- Kutser, T.; Vahtmäe, E.; and Metsamaa, L.** (2005). Spectral library of macroalgae and benthic substrates in Estonian coastal waters. *Proc. Estonian Academy of Science. Biology and Ecology*, 55, 4, 329.340
- Lee, Y.-S.; Park, S.-H.; Cho, Y.-H.; Lee, W.-J, Jung, H.-S.; Lee, M.-J., and Kim, S.-H.,** (2019). Classification of halophytes from airborne hyperspectral imagery in Ganghwa Island, Korea using multilayer perceptron artificial neural network. *In: Jung, H.-S.; Lee, S.; Ryu, J.-H., and Cui, T. (eds.), Advances in Remote Sensing and Geoscience Information Systems of Coastal Environments. Journal of Coastal Research*, Special Issue No. 90, pp. 243-250. Coconut Creek (Florida), ISSN 0749-0208.
- Lombard, F. and Andrieu, J.** (2021). Mapping mangrove zonation changes in Senegal with Landsat imagery using an OBIA approach combined with linear spectral unmixing. *Remote Sensing*, 13(10), 1961.
- Mason, R.L.; Gunst, R.F.; and Hess, J.L.** (2003). Statistical design and analysis of experiments with applications of engineering and science, 2nd edition, John Willey and Sons Hoboken, New Jersey, USA.
- Mohammed,** (2023). Mapping and environmental evaluation of Mangroves habitats along the southern coast of Egyptian Red Sea. Research project reports. Marine Science Departments. NARSS.
- PERSGA (The Regional Organization for the Conservation of the Environment of the Red Sea and Gulf of Aden)** (2004). *Status of Mangroves in the Red Sea and Gulf of Aden*.

- Rahmandhana, A.D.; Kamal, M. and Wicaksono, P.**, (2022). Spectral Reflectance-Based Mangrove Species Mapping from WorldView-2 Imagery of Karimunjawa and Kemujan Island, Central Java Province, Indonesia. *Remote Sens.* *14*, 183. <https://doi.org/10.3390/rs14010183>
- Sanjoto, T.B.; Husna, V.N. and Sidiq, W.A.B.N.**, (2022). Spectral angle mapper algorithm for mangrove biodiversity mapping in Semarang, Indonesia. *Visions for Sustainability*, *18*, 173-190.
- Sabeel, R.**, (2015). Variation in distribution of Sudanese mangroves and their ecological significance for benthic fauna. MSc. Fac. Sci., Uni. Gent. P 290
- Shaltout KH.; El-Bana MI. and Eid EM.** (2018). Ecology of the mangrove along the Egyptian Red Sea Coast. Lambert Academic Publishing, Saarbrücken
- Spalding, M.** (2010). World Atlas of Mangroves. London: Routledge.
- Shaltout, K.H.; Khalaf-Allah, A. and El-Bana, M.**, (2005). Environmental Characteristics of the Mangrove Sites along the Egyptian Red Sea Coast Assessment and Management of Mangrove Forests in Egypt for Sustainable Utilization and Development A Project Funded by ITTO (JAPAN) and SUPERVISED BY MALR / MSEA / EEAA. Report. <https://doi.org/10.13140/RG.2.1.3879.1522>
- Taureau, F.; Robin, M.; Proisy, C.; Fromard, F.; Imbert, D. and Debaine, F.** (2019). Mapping the Mangrove Forest Canopy Using Spectral Unmixing of Very High Spatial Resolution Satellite Images. *Remote Sens.* *11*, 367. <https://doi.org/10.3390/rs11030367>
- Thayn, J. B.** (2020). 'Monitoring Narrow Mangrove Stands in Baja California Sur, Mexico Using Linear Spectral Unmixing'. *Marine Geodesy*, *43*(5), pp. 493–508. doi: 10.1080/01490419.2020.1751753.
- Tharwat A.** (2018). Classification assessment methods. *Applied Computing and Informatics.* *17*: 168–192. [doi:10.1016/j.aci.2018.08.003](https://doi.org/10.1016/j.aci.2018.08.003).
- Tran, T.V.; Reef, R. and Zhu, X.** (2022). A Review of Spectral Indices for Mangrove Remote Sensing. *Remote Sens.*, *14*, 4868. <https://doi.org/10.3390/rs14194868>
- Tukey, J.W.** (1977). Exploratory Data Analysis. Addison-Wesley, Reading, MA
- Wang, H.; Zhang, J.; Wu J. and Yan, Z.** (2017). "Research on mangrove recognition based on hyperspectral unmixing,". *IEEE International Conference on Unmanned Systems (ICUS)*, Beijing, China, 2017, pp. 298-300, doi: 10.1109/ICUS.2017.8278358.
- Wang LE., and Sousa W. P.**, (2009). Distinguishing mangrove species with laboratory measurements of hyperspectral leaf reflectance. *International Journal of Remote Sensing*, Vol. *30*, No. 5, 1267–1281.
- Witsen, D.** (2012). Mangrove Restoration and Management in Djibouti. MSc. Natural Resources. Virginia Polytechnic Institute and State University. P 28
- Xu, Y.; Wang, J.J.; Xia, A.Q.; Zhang, K.Y.; Dong, X.Y.; Wu, K.P. and Wu, G.F** (2019). Continuous wavelet analysis of leaf reflectance improves classification accuracy of mangrove species. *Remote Sens.* *11*, 254.
- Zhu J.; He W.; Yao J.; Yu Q.; Xu C.; Huang H.; Mhae B. and Jandug C.** (2020). Spectral Reflectance Characteristics and Chlorophyll Content Estimation Model of *Quercus aquifolioides* Leaves at Different Altitudes in Sejila Mountain. *Applied Sciences.* *10*(10):3636. <https://doi.org/10.3390/app10103636>